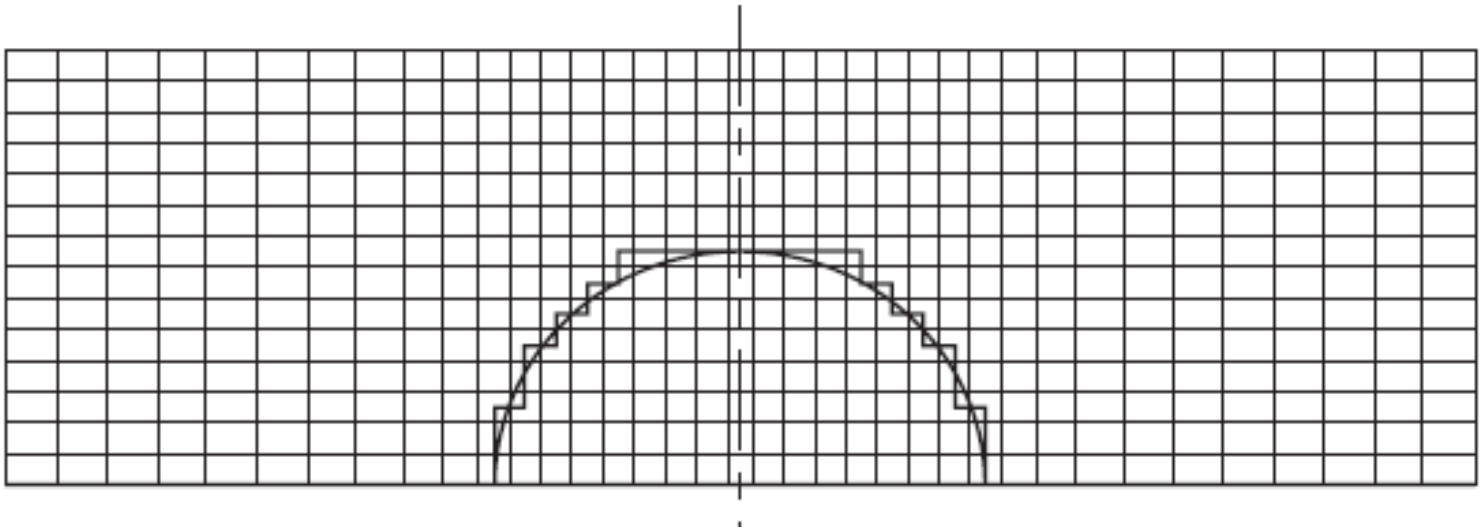

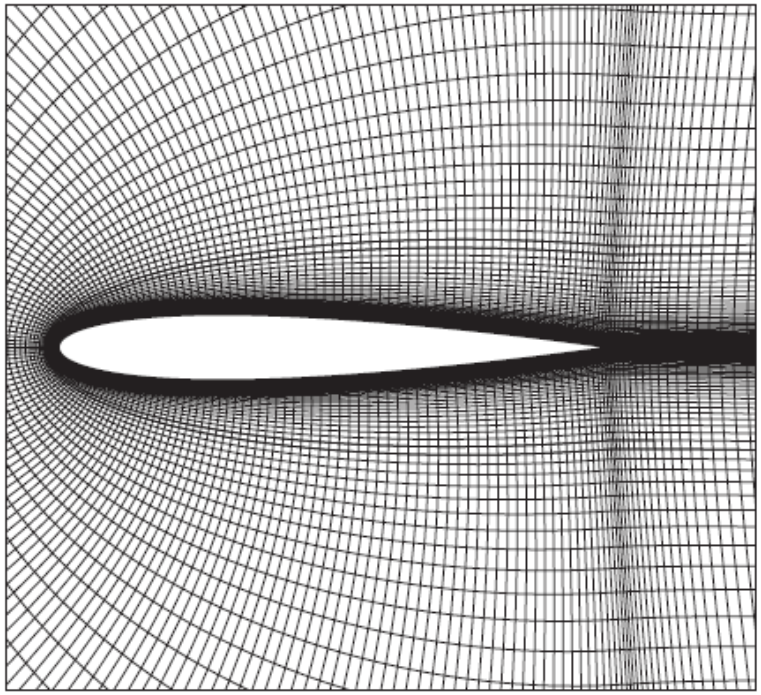

Figure 11.2 An example of an orthogonal curvilinear mesh for calculating flow around an aerofoil
Source: Haselbacher (1999)

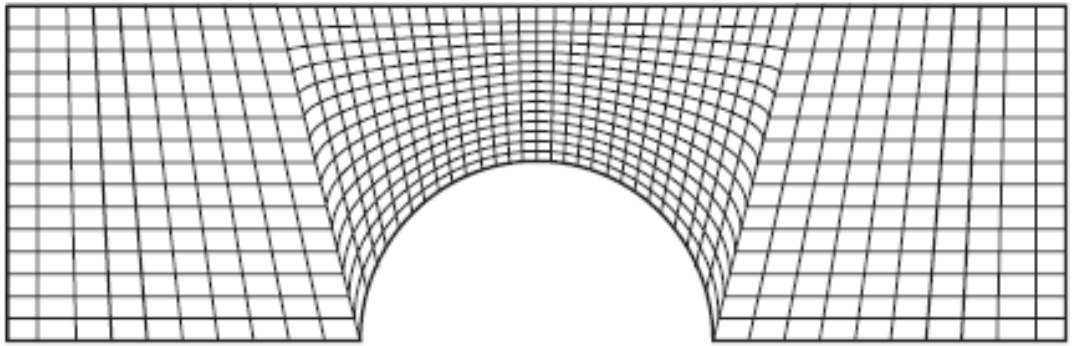

Figure 11.3 Use of a non-orthogonal body-fitted grid arrangement for the prediction of flow over a cylinder

Figure 11.4 Flow over a heat exchanger tube bank (only a part shown)

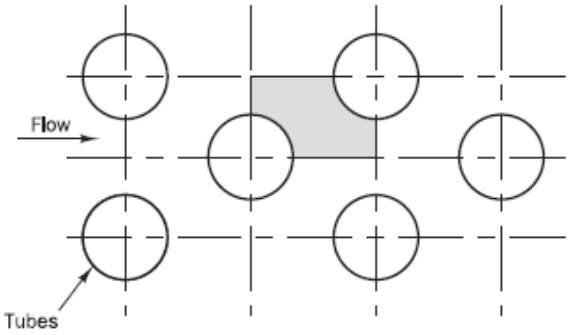

Figure 11.5 (a) Cartesian grid using an approximated profile to represent cylindrical surfaces; (b) predicted flow pattern using a 40×15 Cartesian grid

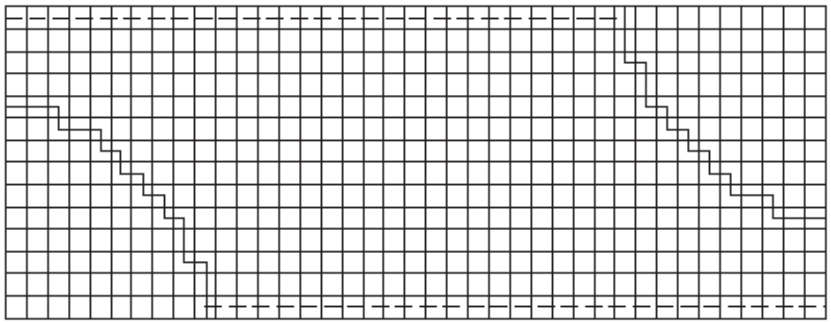

(a)

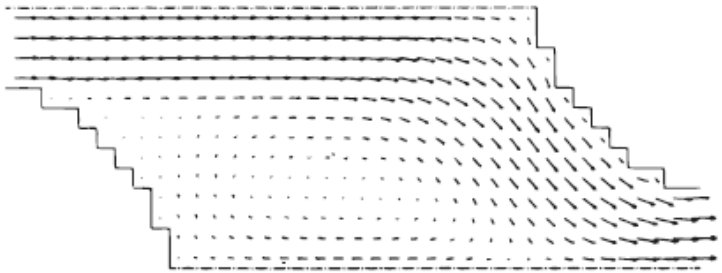

(b)

Figure 11.6 (a) Non-orthogonal body-fitted grid for the same problem; (b) predicted flow pattern using a 40×15 structured body-fitted grid

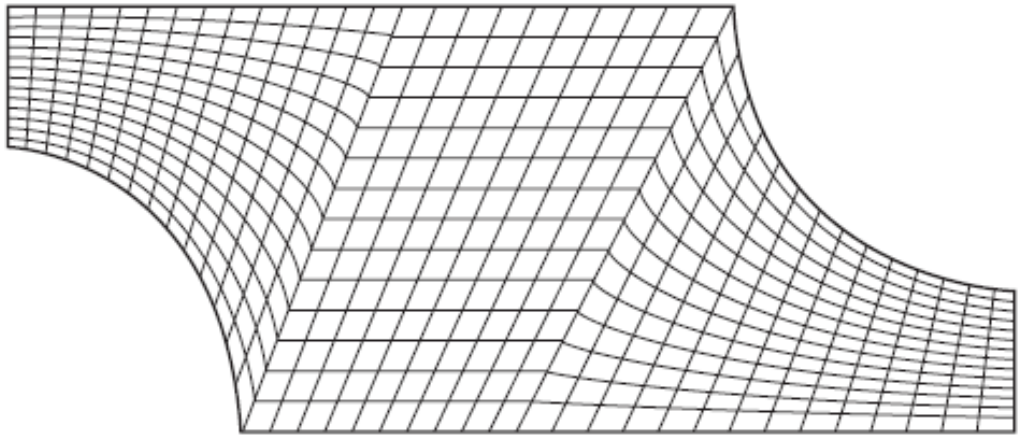

(a)

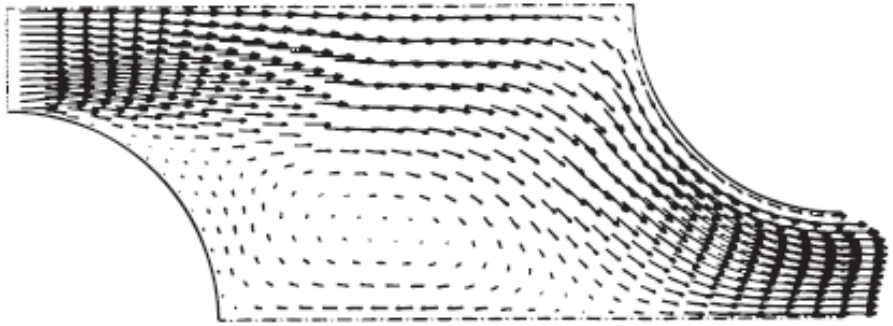

(b)

Figure 11.7 Mapping of physical geometry to computational geometry in structured meshes: (a) physical grid in x, y co-ordinates; (b) the mapped structure for (a) in the computational domain

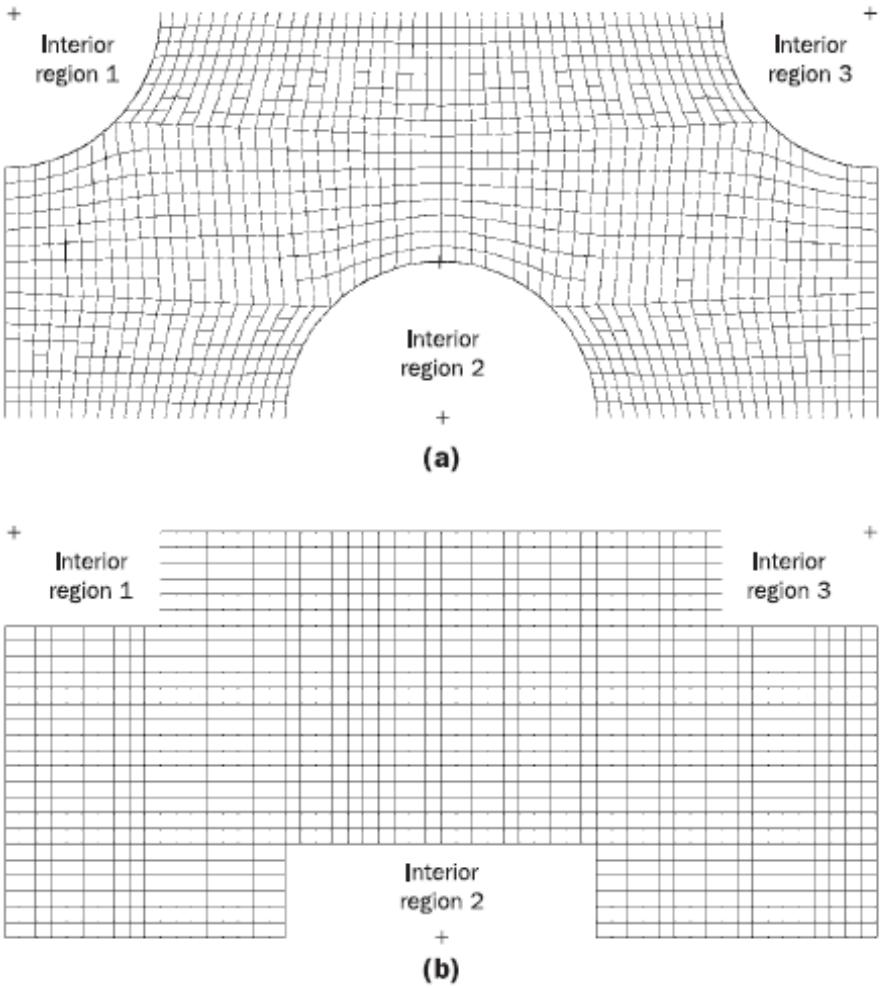

Figure 11.8 A structured non-orthogonal mesh for a pent-roof i.c. engine geometry

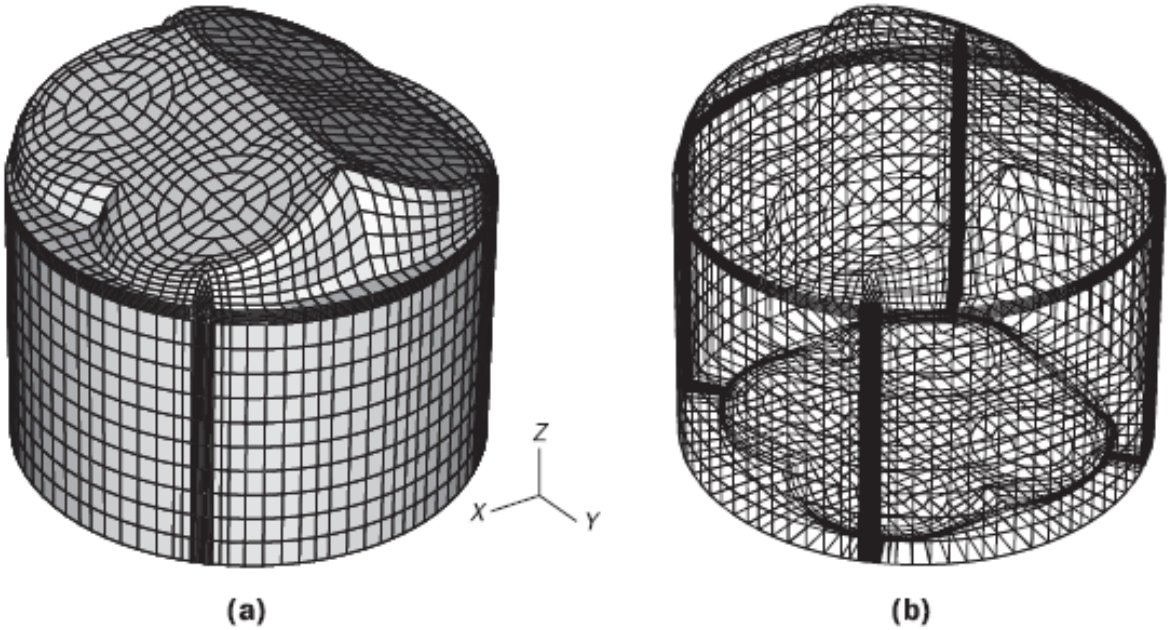

Figure 11.9 Block-structured mesh for a transonic aerofoil. Inset shows cut cells near aerofoil surface. Also note additional grid refinement in the flow region to capture a shock above the aerofoil
Source: Haselbacher (1999)

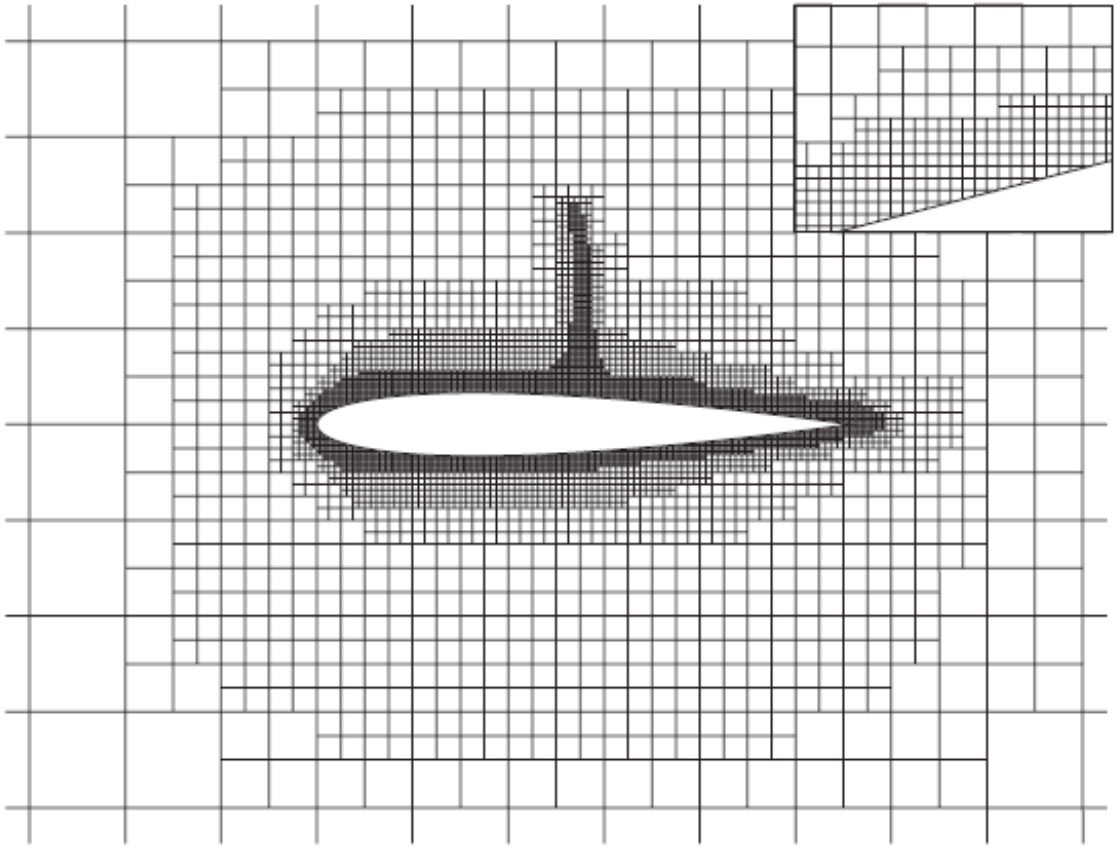

Figure 11.10 Block-structured mesh arrangement for an engine geometry, including inlet and exhaust ports, used in engine simulations with KIVA-3V

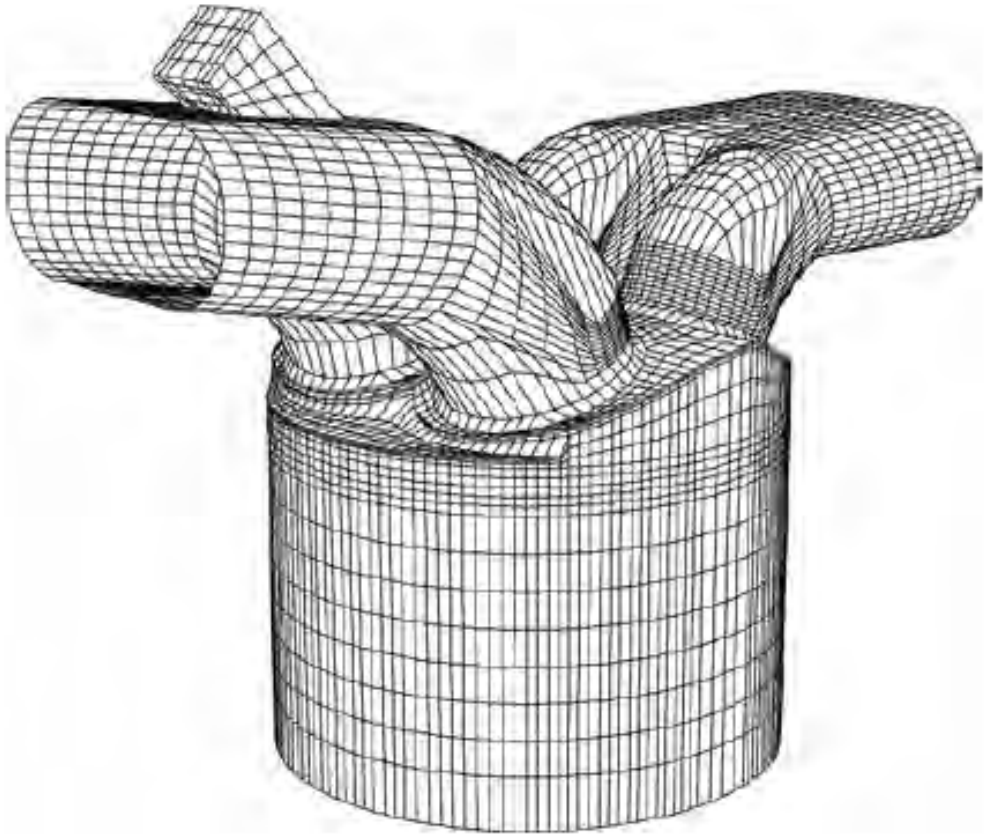

Figure 11.11 A triangular grid for a three-element aerofoil
Source: Haselbacher (1999)

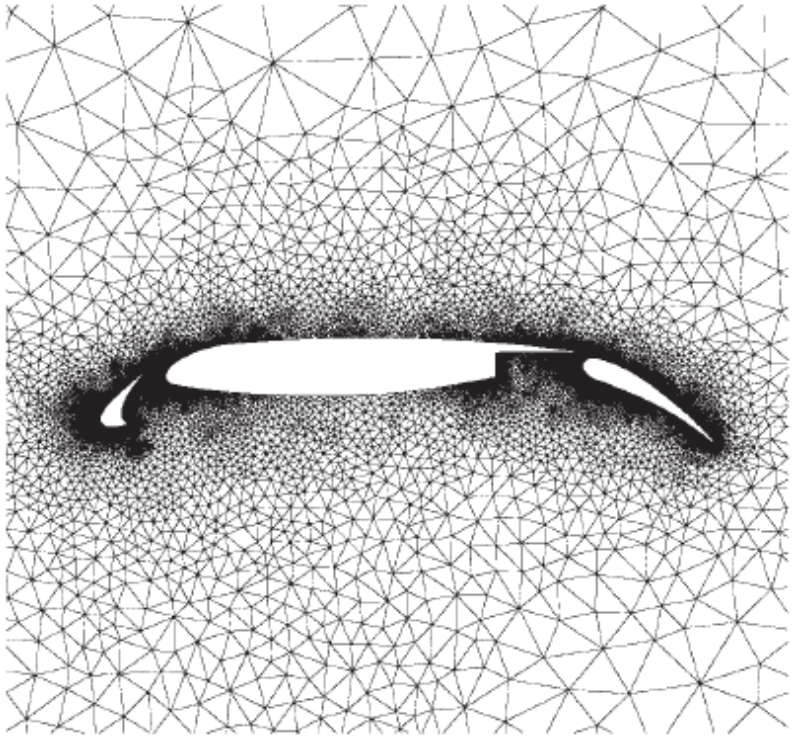

Figure 11.12 An example of an unstructured mesh with mixed elements

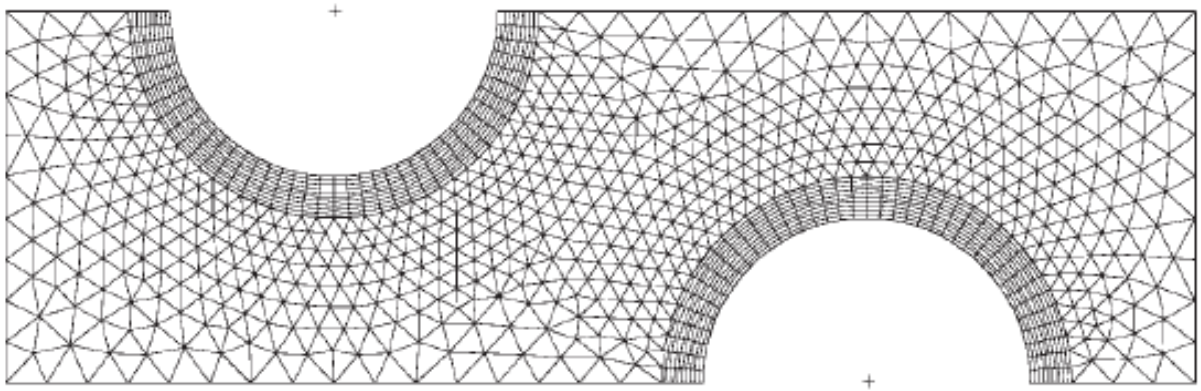

Figure 11.13 Control volume construction in 2D unstructured meshes: (a) cell-centred control volumes; (b) vertex-based control volumes

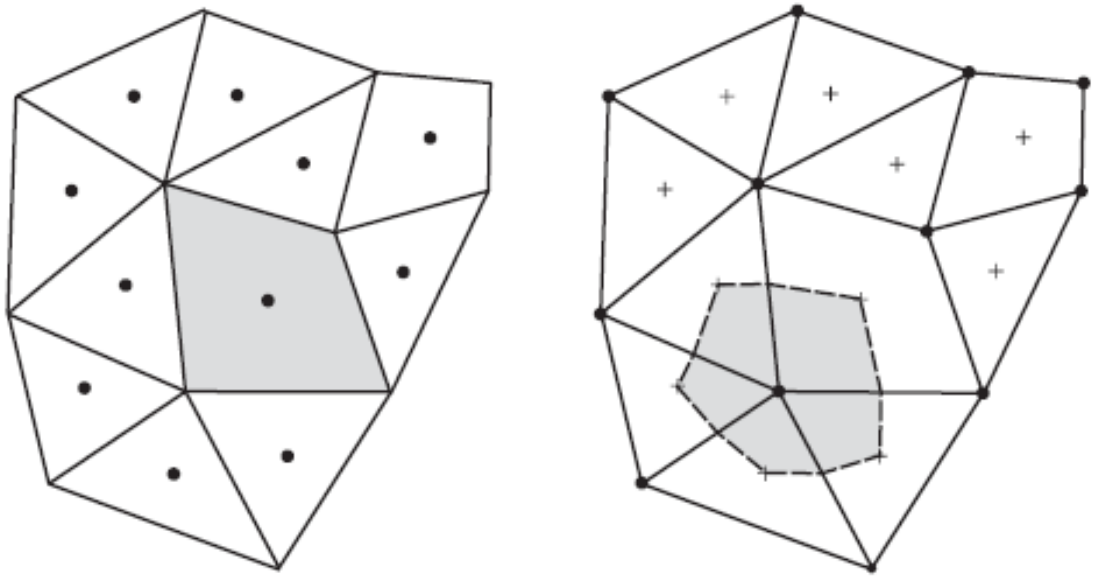

Figure 11.15 Cell-centred control volume arrangement

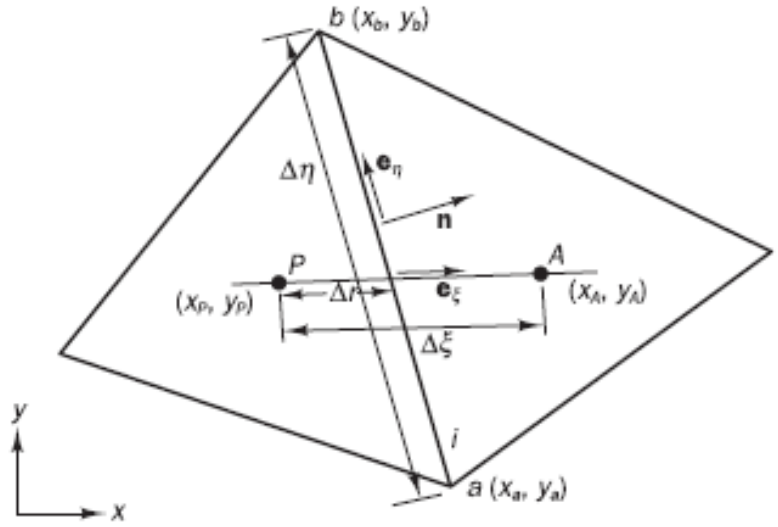

Figure 11.16 A face of a control volume and the normal unit vector

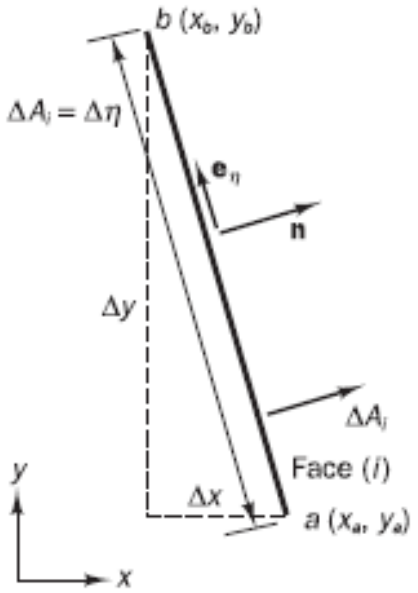

Figure 11.19 A control volume and its neighbour nodes